



Modeling Medium Size ($M_w \sim 5.0$) Teleseismic Earthquakes Using Path Calibration

R. Chu¹, S. Ni², and D. V. Helmberger¹

California Institute of Technology¹ and URS Group, Inc.²



Abstract

Precise determination of earthquake origin time, hypocenter, focal mechanism, and magnitude is a major theme for seismic monitoring community. For large earthquakes ($M_w > 5.5$), there are many methods of inversion, i.e. Centroid Moment Tensor (CMT), to invert those properties. For example, the Cut and Paste (CAP) method can use as few as two stations to retrieve earthquake location and mechanism using long-period regional waveform data. But for medium-size ($M_w \sim 5.0$) earthquakes, their regional waveforms are very limited in some region, such as Iran. Fortunately their teleseismic data are recorded globally, and can be used to determine focal mechanism and magnitude at relative high frequency.

In this poster, we introduce a new method (CAPt) to determine focal mechanism and magnitude of medium size ($M_w \sim 5.0$) earthquakes using teleseismic waveforms. This method uses a grid-search algorithm to minimize misfits between observed data and synthetic seismograms in the frequency range of 0.8–2.0 Hz in depth, magnitude, and mechanism domain, similar to the CAP method. At this frequency range, a significant problem is that the resulting focal mechanism is very sensitive to earthquake depth, and sometimes the best-fit mechanism is reverse due to unknown arrival times. Therefore we use CAPt to determine source properties for an earthquake with high signal-to-noise ratio (SNR). The most important output is the time delay relative to 1D background velocity model for each recording station. We use these delays to calibrate the travel-time effect of ray path due to 3D heterogeneity. For highly clustered aftershocks, we determine their arrival times by adding their delays accordingly. Then mechanism and magnitude can be determined by CAPt.

We applied this method to four events in southern Iran and retrieved their focal mechanism. The results suggest that this method can precisely determine earthquake mechanism. We also calculated amplitude amplification factor (AAF) for each station, which is treated as the amplitude calibration of the ray path. It turns out that AAF is independent of earthquake mechanism, and can be used for high resolution studies, directivity etc.

Introduction

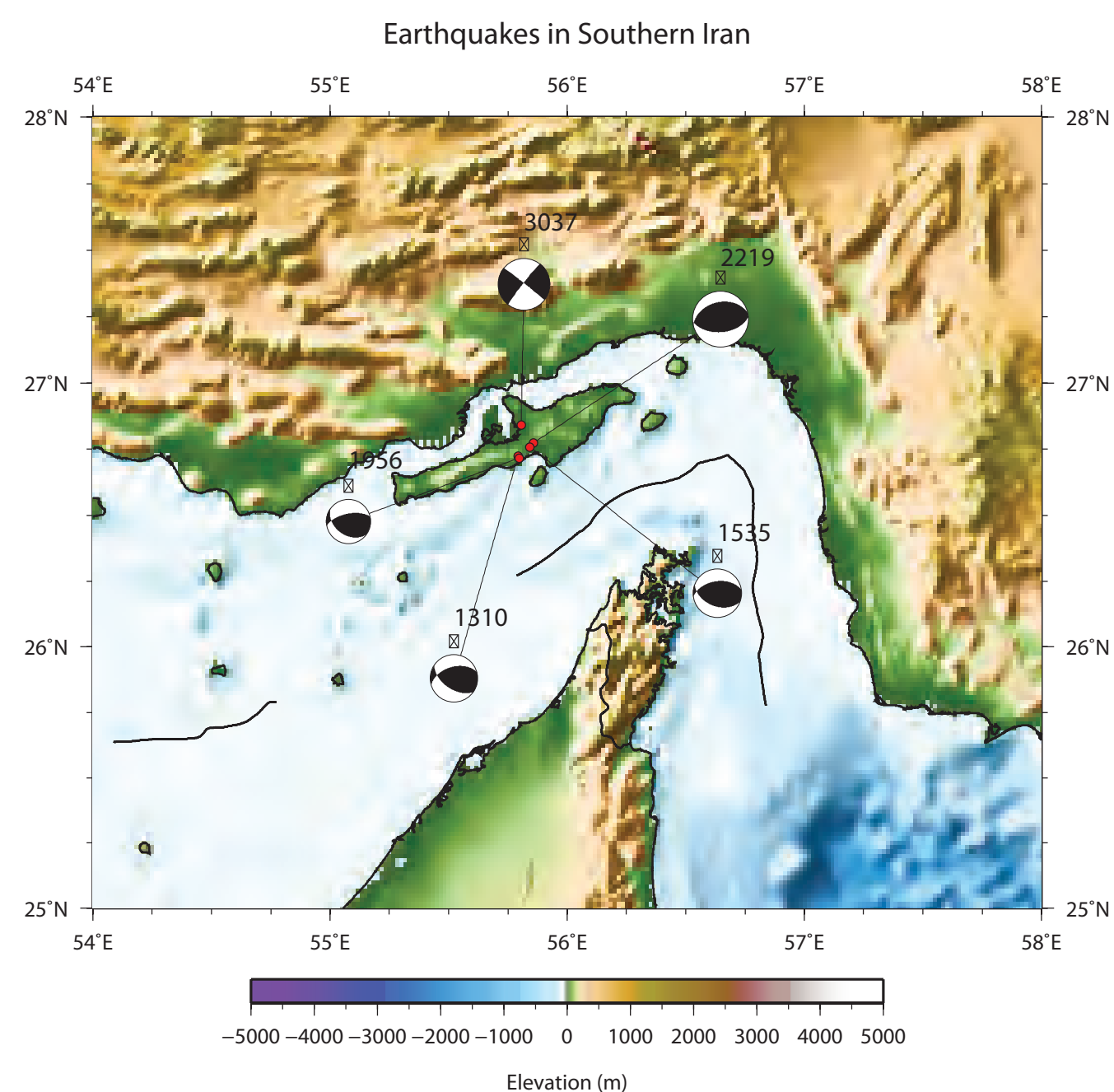


Figure 1: Five earthquakes in southern Iran used in this study. The focal mechanisms are from CMT catalog.

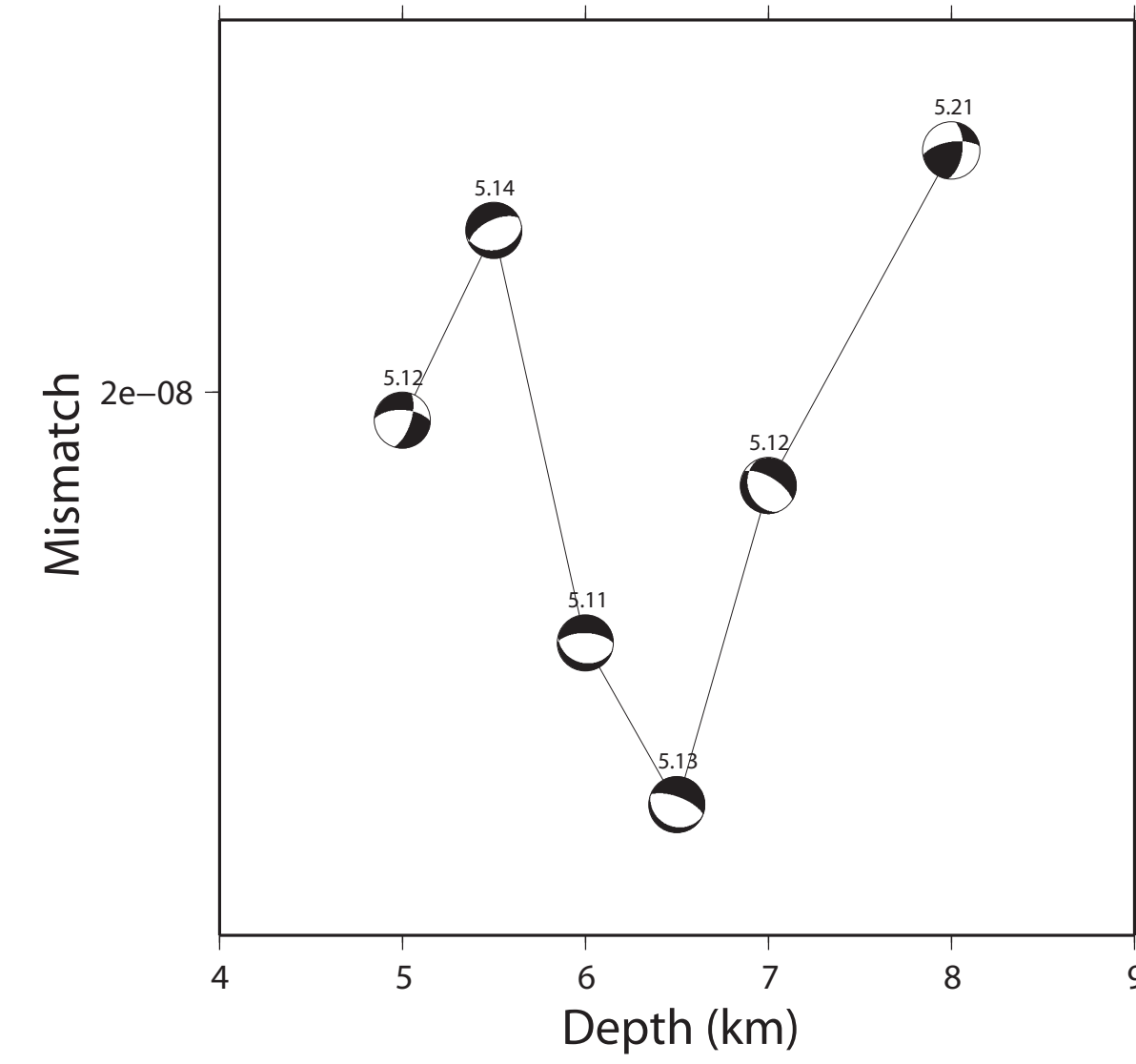


Figure 2: Misfits between observed and synthetic seismograms as a function of earthquake depth for event 1956. Note that the mechanism changed rapidly from normal faulting at 7 km to thrusting at 8 km. The best-fit solution at 6.5 km is reverse to the mechanisms suggested by the CMT catalog in Figure 1 for long periods.

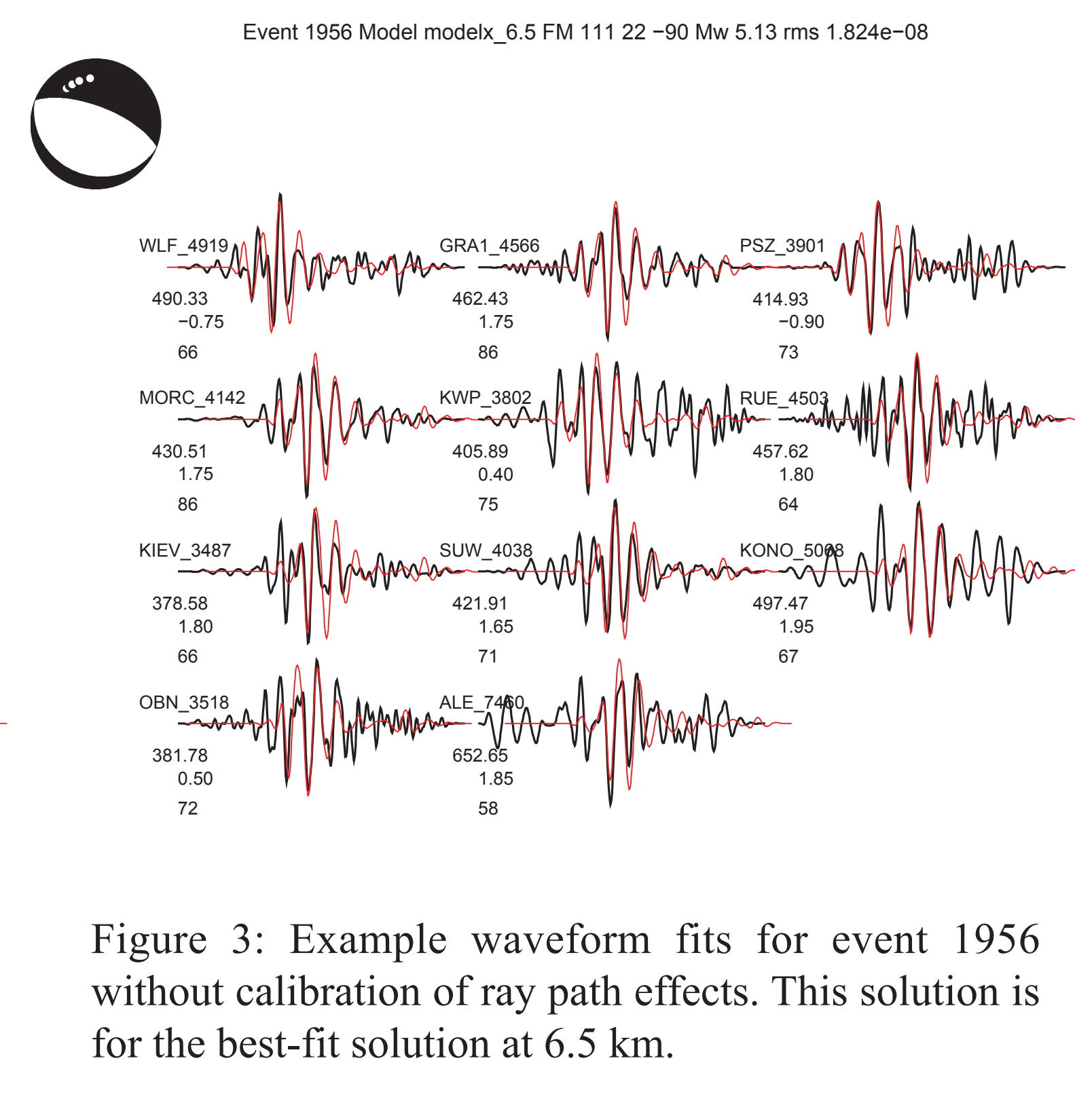
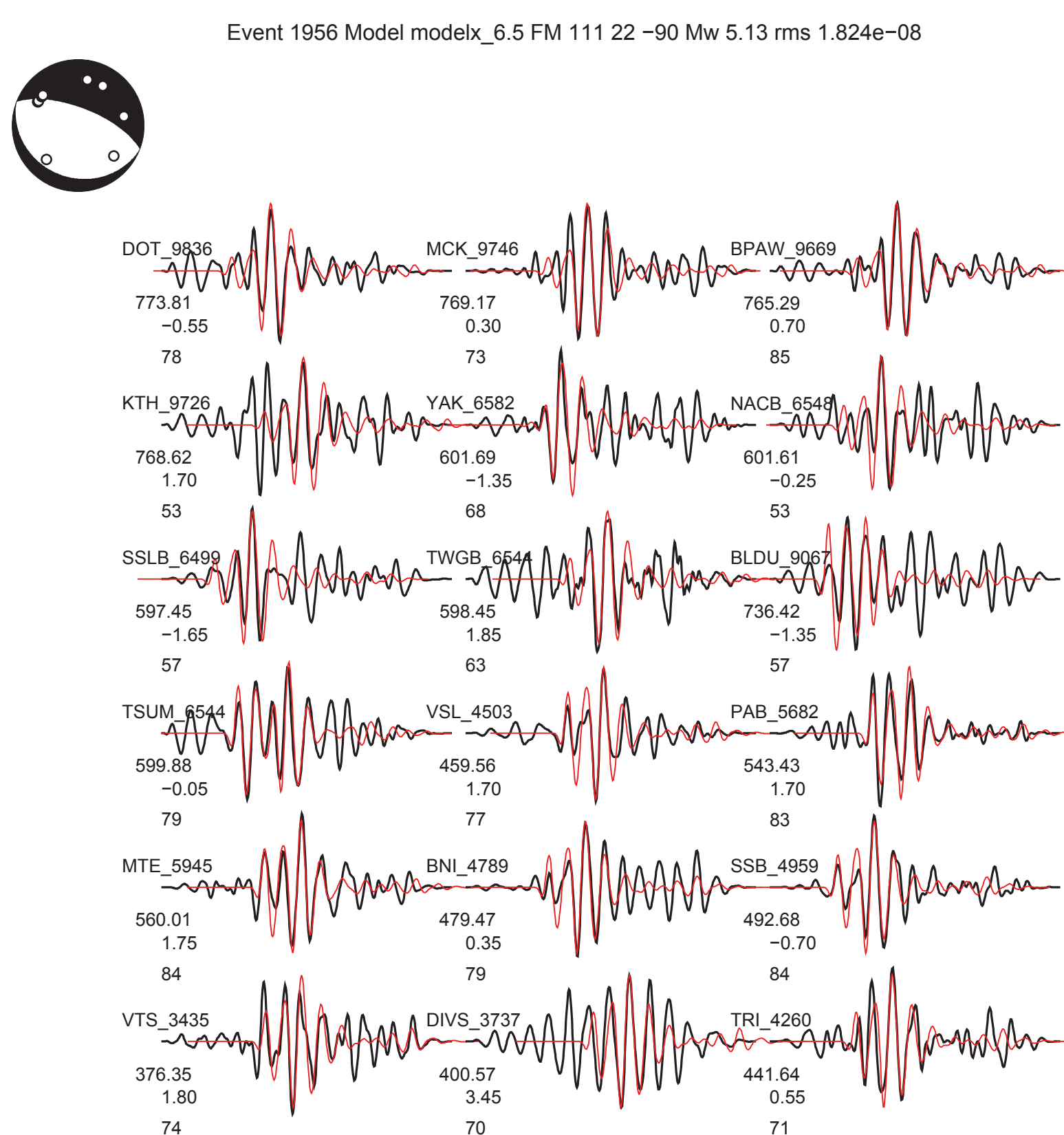


Figure 3: Example waveform fits for event 1956 without calibration of ray path effects. This solution is for the best-fit solution at 6.5 km.

Travel-time calibration

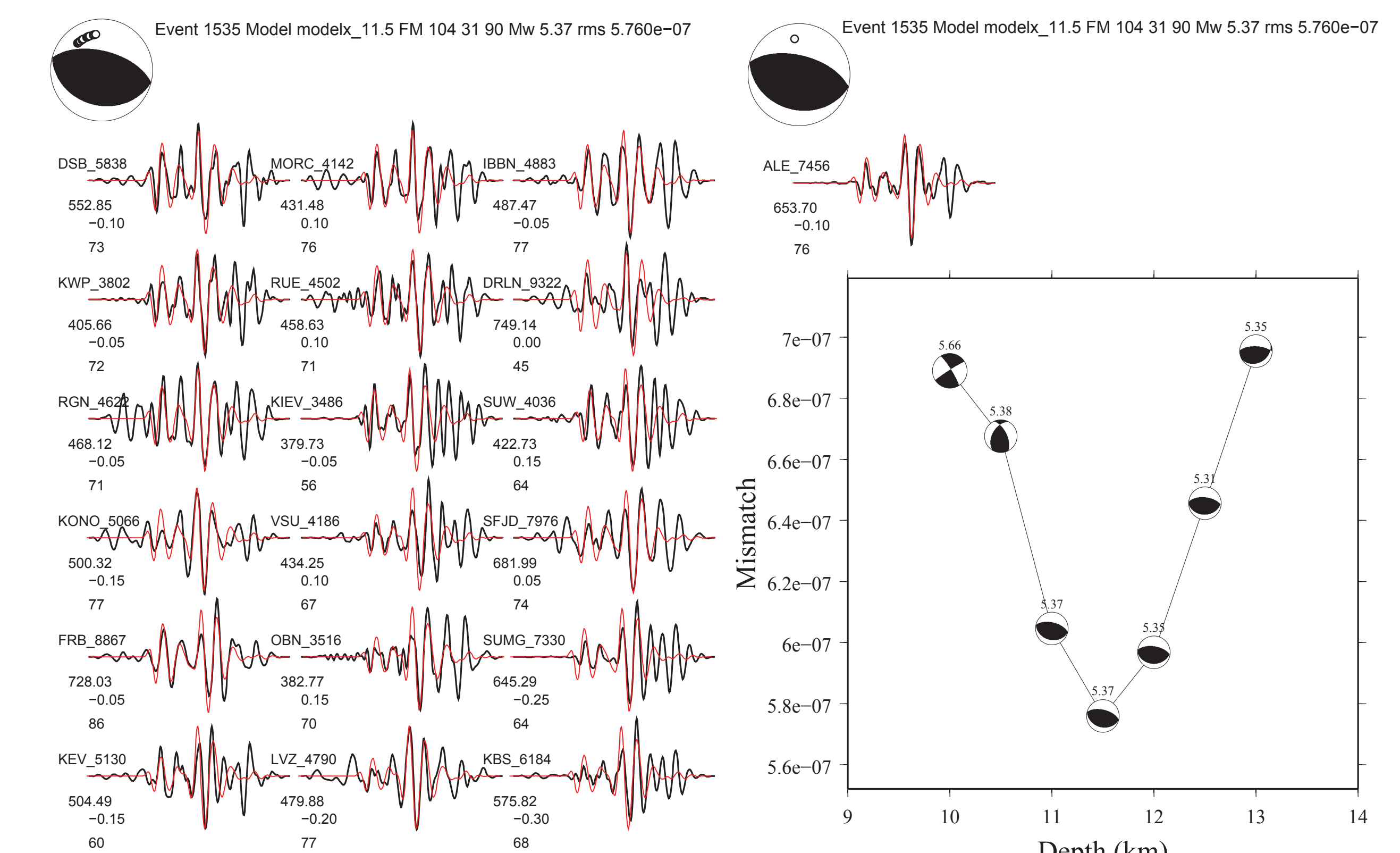
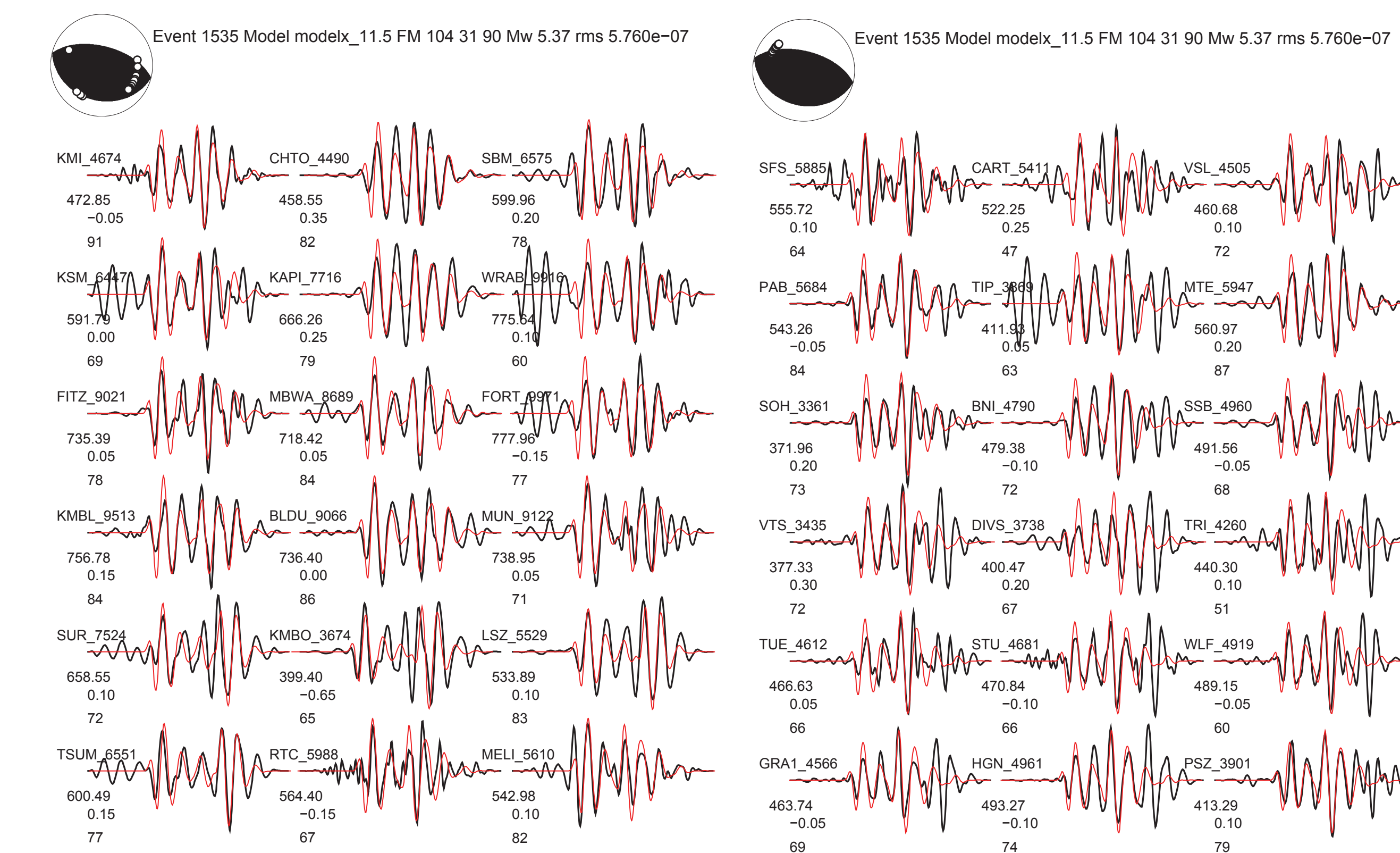
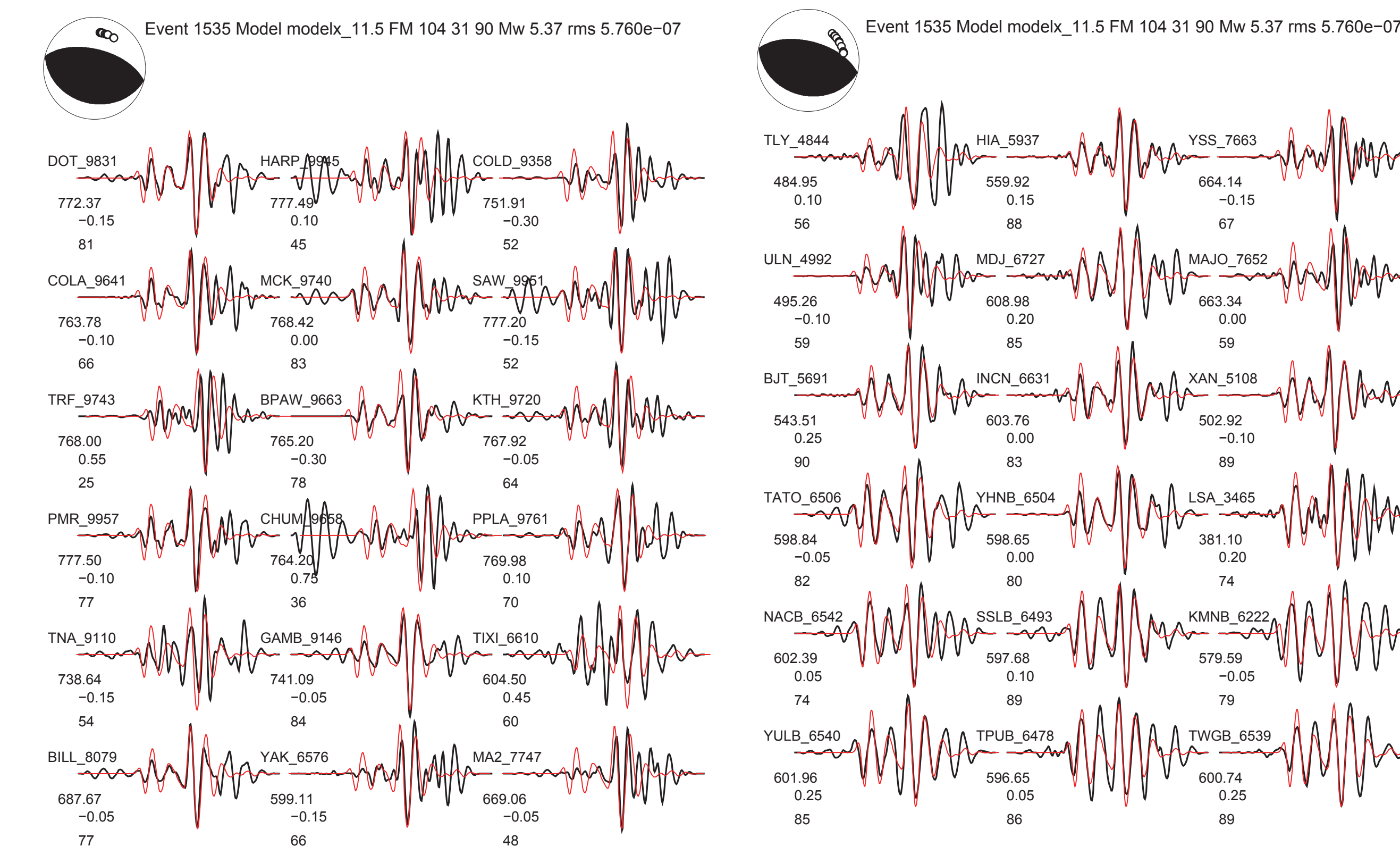


Figure 4: Waveform fits for event 1535 without calibration of ray path effect and misfits as a function of depth. This solution is for the best-fit solution at 11.5 km. Numbers before each seismogram is station name and distance, arrival time, time shift, and cross-correlation coefficient. Travel-time delays can be calculated using the arrival times and predictions of 1D background velocity model.

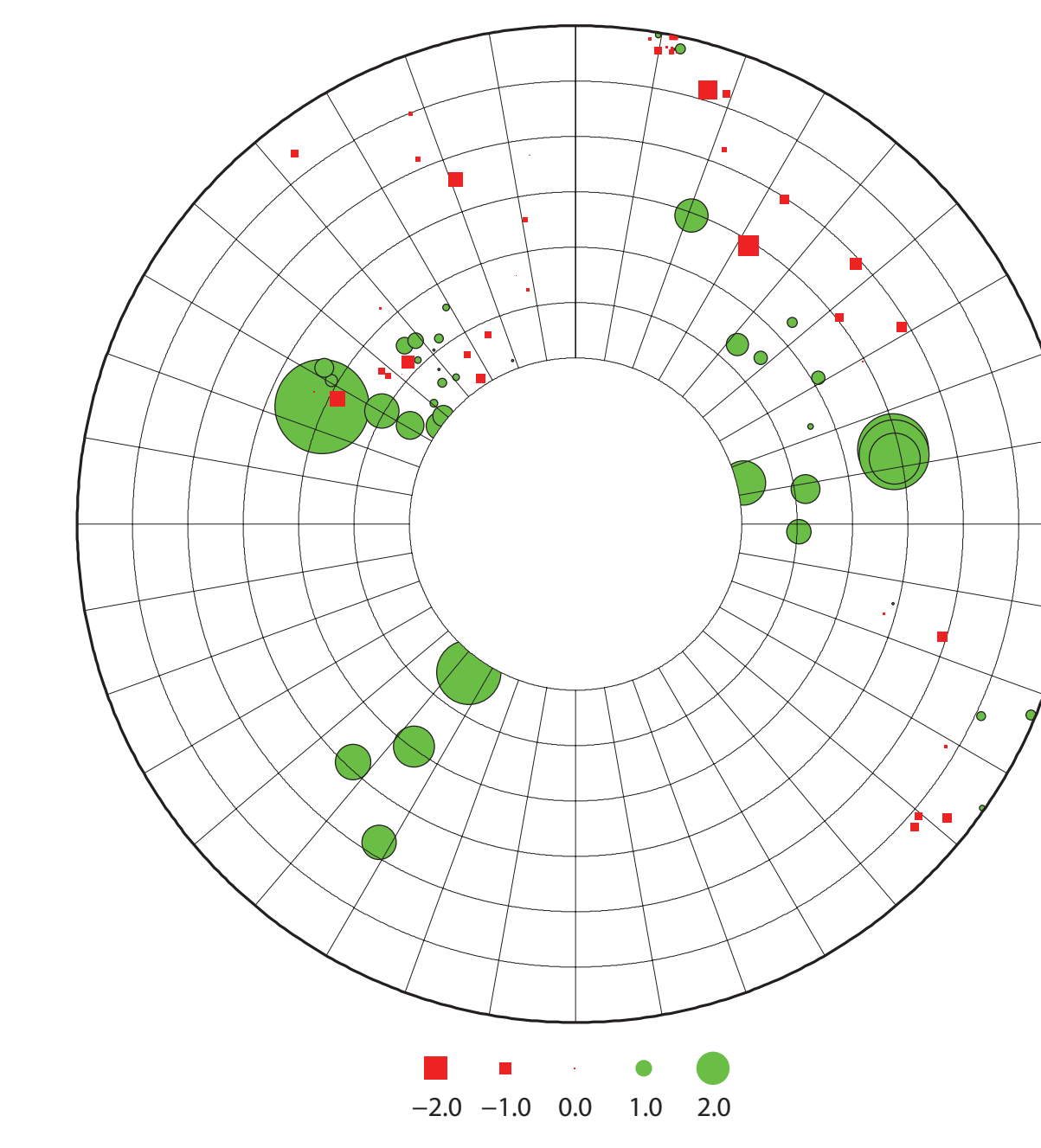


Figure 5: Travel-time delays for event 1535 as a function of azimuth and distance. The scale shows amplitude of the residuals.

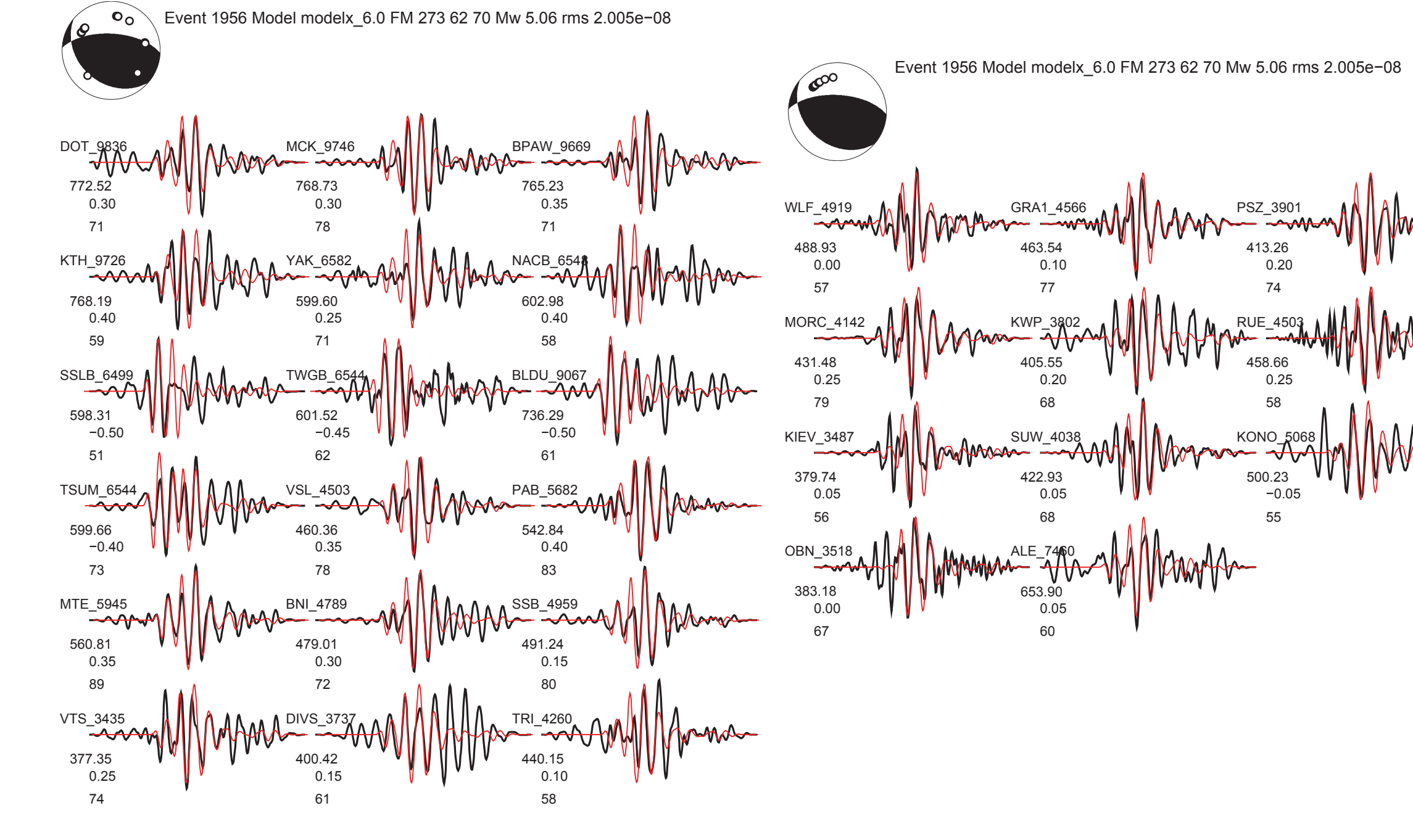


Figure 6: Waveform fits for event 1956 and misfit as a function of depth after correcting travel-time delays for each station. The mechanism changes smoothly from strike-slip faulting at 5 km to thrusting at 6 km, and to normal faulting at 8 km.

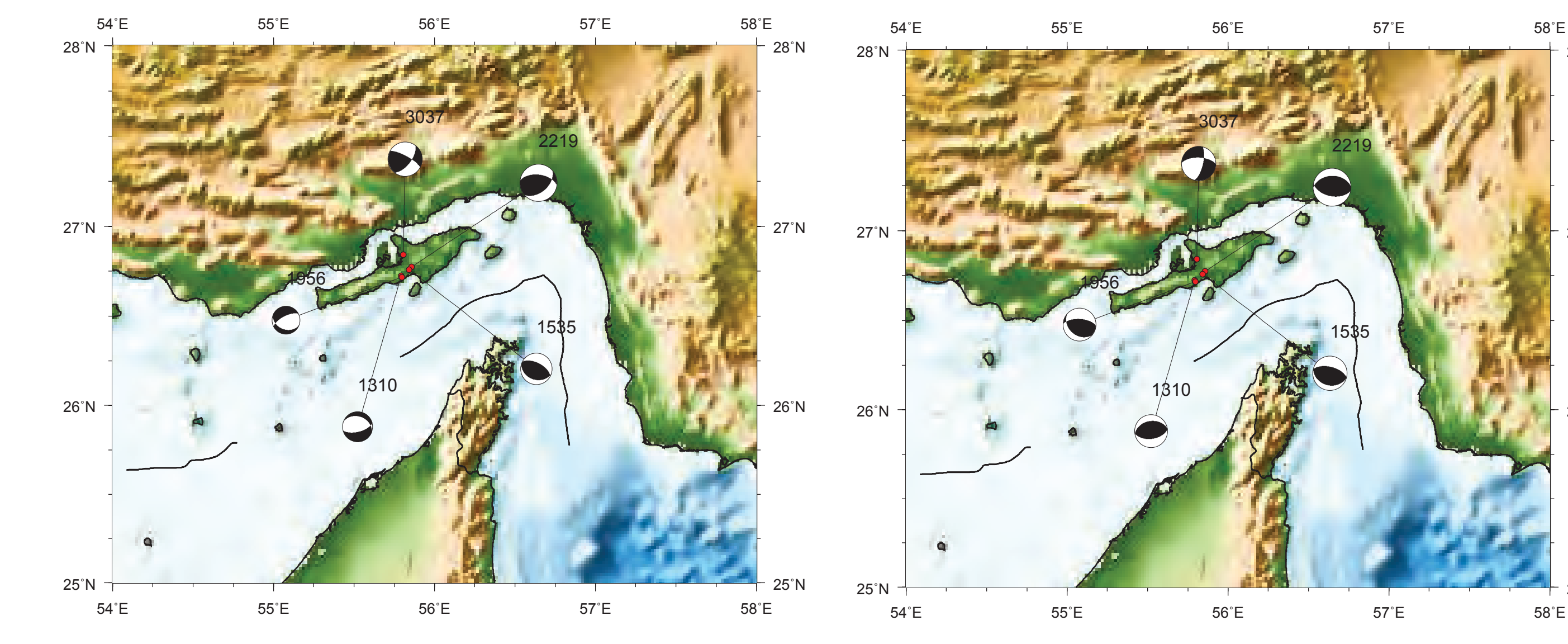


Figure 7: Comparison of earthquake mechanisms from modeling waveforms at regional (left) and teleseismic (right) distance. The regional waveform modeling is done using CAP by A. Rodgers (Rodgers et al., 2008). Event 2219 is a $M_w \sim 5.9$ main event. Calibration event 1535 has the same mechanism as the main shock, and they agree with the mechanisms from other sources. For event 1310 and 1956, regional waveform modeling yields normal faulting. Since they are within 10 km of the main shock, it is more reasonable to have similar mechanism as the main event. By comparing all mechanisms to those from CMT catalog in Figure 1, it can be concluded that CAPt can precisely recover focal mechanisms.

Amplitude Calibration, the amplitude amplification factor (AAF)

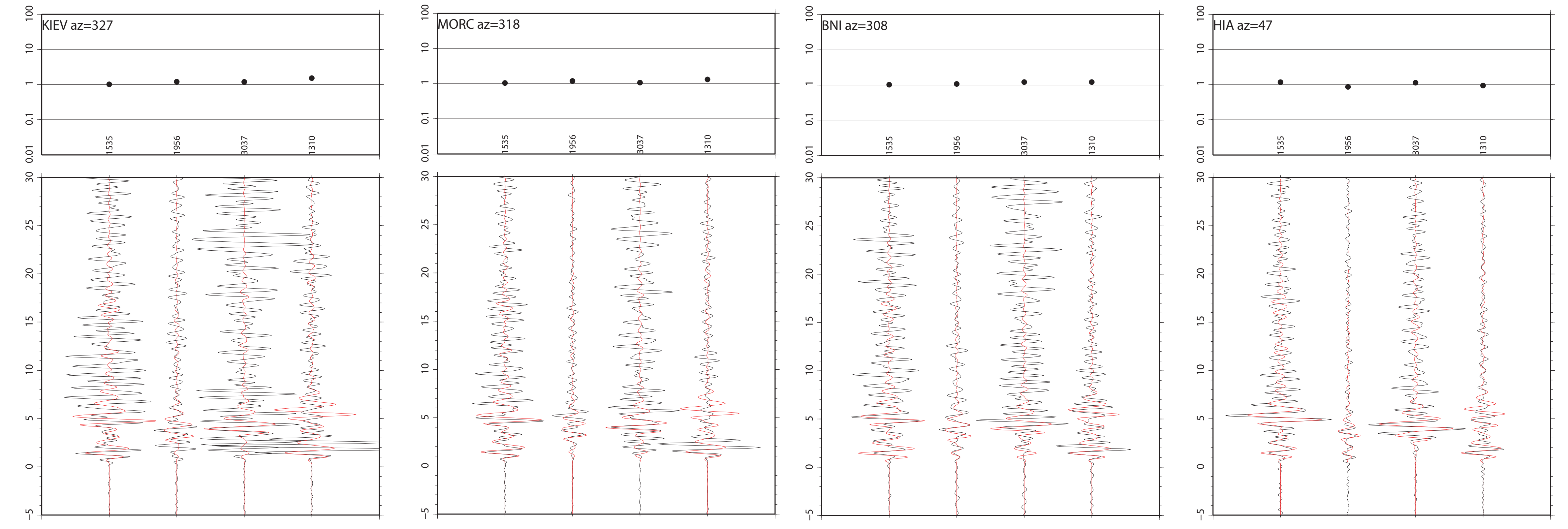


Figure 8: AAFs (top) and waveform fits (bottom) for station KIEV, MORC, BNI, and HIA. The AAFs are the ratio of peak-to-valley values between observed and synthetic waveforms. Synthetic and observed waveforms at these stations have high cross-correlation coefficient. It is obvious that AAFs are independent of earthquake mechanisms. Hence they can be used as the amplitude calibration of the ray path effect.

Conclusion

1. At frequency range of 0.8–2.0 Hz, the mechanism is hard to determine from modeling teleseismic waveforms without travel-time corrections since the initial polarity is difficult to determine.
2. AAFs are independent of focal mechanisms and can be used as the amplitude calibration of the ray path effect.
3. By combining the travel-time and amplitude calibration, earthquake mechanism and magnitude can be precisely determined from modeling teleseismic waveforms. Such precision can now be used to conduct secondary source effects, directivity, etc as in regional studies, Tan and Helmberger (2006).